https://doi.org/10.5194/egusphere-2024-1169
Preprint. Discussion started: 13 May 2024

Projected changes of Active layer thickness over permafrost under 1.5~5.0°C climate warming on the Qinghai-Tibet Plateau

Zhenjie Li[1,2,3,6], Buda Su[2], Jinlong Huang[2], Peni Hausia Havea[2], Runhong Xu[4], Cheng Jing[1,2,3], Yu Gong[1,2,3], Tong Jiang[2,5]

[1] State Key Laboratory of Desert and Oasis Ecology, Xinjiang Institute of Ecology and Geography, Chinese Academy of Sciences, Urumqi 830011, China
[2] Research Institute of Climatic and Environmental Governance /Institute for Disaster Risk Management, School of Geographical Science, Nanjing University of Information Science & Technology, Nanjing 210044, China
[3] University of Chinese Academy of Sciences, Beijing 100011, China
[4] Qinghai Normal University, Xining , China
[5] Jiangsu Second Normal University, Nanjing 210013, China
[6] Lincang Meteorological Bureau, Lincang Yunnan 677099, China

First authors equally contributions: Zhnejie Li (lizhenjie17@163.com) and Buda Su (subd@nuist.edu.cn)

Correspondence: Jinlong Huang (huangjl_2012@163.com) and Tong Jiang (jiangtong@nuist.edu.cn)

Abstract. Permafrost degradation and active layer thickness (ALT) changes on the Qinghai-Tibetan Plateau (QTP) are caused by soil temperature increases under the continuous increase in global temperature. Therefore, the soil zero-degree layer can be used as an index to investigate the changes in permafrost and the ALT. The observed and projected permafrost and ALT were estimated by the summer soil zero-degree layer using soil temperature data from weather stations and the Coupled Model Intercomparison Project Phase 6 (CMIP6). The results revealed that the ALT is deeper in summer (e.g., July), indicating that the melting capacity increases. The CMIP6-simulated and observed soil temperatures are consistent in the vertical direction across the QTP, but the model results exhibit significant cold deviations. The average ALT on the Qinghai–Tibet Plateau was approximately 3.75 m (range of 1.10~15.91 m) during 1961-1990 and increased to 5.77 m (range of 1.72~13.53 m) during 1991-2022, an increase of 53.9%. The observed ALT were >6 m in the southeastern QTP area, such as east and south of Shigatse and Lhasa, where it was <3 m in the western Pamir Plateau, near Gaize, north of Qamdo in the northeast and east of Golmud, and other central and northern regions, where the values were 3-6 m. The ALT will continue to increase under the four Shared Socioeconomic Pathways (SSPs), especially when the radiative forcing level is high, and they will increase by 39.6% under SSP5-8.5 by the end of the 21st century. The regional average of ALT will increase by 5.4% for every 0.5°C increase in global warming levels, increasing from 10.6% to 47.1%. A small change (e.g., <20%) in the coverage area of the ALT will occur, decreasing from 1,424,735 km^2 to 13,682 km^2. However, the coverage area with a depth increase of more than 100% will increase from 0 to 401,433 km^2. The regions where the ALT slightly increases are primarily distributed in the northeast, east and southeast regions of the QTP, and the region where the ALT dramatically

https://doi.org/10.5194/egusphere-2024-1169
Preprint. Discussion started: 13 May 2024

increases is in the western region, where there is concentrated permafrost.

1 Introduction

Because of global warming, permafrost temperatures in polar and high mountain regions have increased to new high levels, increasing by 0.29 ℃±0.12 ℃ observed from 2007 to 2016 (SROCC, 2019). The annual mean surface temperature of the Qinghai-Tibetan Plateau (QTP) has reached a threshold of 1.5 ℃ relative to that in the preindustrial period (1850-1900), resulting in significant permafrost degradation (Chen et al., 2022). The degradation of QTP permafrost is mainly manifested by the increase in soil temperature, increase in active layer thickness (ALT), increase in the lower limit of permafrost, and degradation of permafrost, which becomes seasonally frozen ground (Cheng et al., 2007; Ran et al., 2018). In the past few decades, the start date of the freezing of seasonally frozen ground on the QTP has been delayed, the end date has advanced, the freezing duration has decreased, and the maximum freezing depth has decreased (Guo et al., 2013; Wu et al., 2015; Ran et al., 2018; Luo et al., 2020; Wang et al., 2020). At present, the area of seasonally frozen ground is approximately 1.447×10^6 km^2 (Cao et al., 2023). The extent of permafrost is projected to shrink in the next few decades on the QTP, specifically, at a greater rate than in the Arctic region (Wang et al., 2022). By the end of the 21st century, more than half of the permafrost area on the QTP will be covered by active layers with a thickness of more than 4 m under the Shared Socioeconomic Pathways (SSP) 5-8.5 (Chen et al., 2023).

The ALT changes are critical to geomorphic processes on the QTP, and the characterization and monitoring of permafrost degradation and its spatial distribution and potential changes are highly important (Wang et al., 2018; Wang et al., 2019a). ALT changes also have important impacts on the surface energy balance, hydrological cycle, ecological processes, carbon flux, landscape processes, and stability of human infrastructure on the QTP (Pang et al., 2009; Wu et al., 2010; Pang et al., 2012; Ding et al., 2017; Ran et al., 2018; Ding et al., 2019; Zhao et al., 2019). Changes in the ALT cause decreases in groundwater and lake levels, the drying of marshes, and the shrinkage of grasslands, while the freeze–thaw cycle of seasonally frozen soil affects the water and heat exchange of the Earth–atmosphere system on the QTP and has an important impact on the East Asian monsoon and even the global climate system (Wang et al., 2002; Cheng et al., 2007; Guo et al., 2017; Cheng et al., 2019). ALT thickening results in the redistribution of water in the soil profile, and the liquid water content in the upper soil layer decreases, while it increases in the deep soil layer (Guo et al., 2012; Xie et al., 2012). ALT thickening increases the risk of geological hazards and causes land subsidence, thereby increasing the cost of adaptation and maintenance infrastructure and resulting in economic losses on the QTP (Guo et al., 2017; Gao et al., 2021; Ran et al., 2022). In the past, soil profile data for the active layer on the QTP were obtained mainly through drilling holes in frozen regions or the use of soil temperature observation data from weather stations to construct soil temperature profiles (Wang et al., 2002; Wu et al., 2010a, 2010b; Wu et al., 2010; Wu et al., 2015; Wang et al., 2019a; Wang et al., 2019b; Luo et al., 2020; Wang et al., 2020; Ran et al., 2021; You et al., 2022). Later, ground penetrating radar (GPR), interferometric synthetic aperture radar (InSAR), manned aerial photographs, unmanned aerial vehicles, high-resolution satellite measurements, and other remote

https://doi.org/10.5194/egusphere-2024-1169
Preprint. Discussion started: 13 May 2024

sensing detection technologies were developed (Cao et al., 2017; Wang et al., 2018; Gao et al., 2021). ALT estimation models, such as the Kudryavtsev formula method, Stefan formula method, accurate development model based on piecewise functions, machine learning method and other mathematical models, have also been established and used for research on the QTP (Pang et al., 2009; Pang et al., 2012; Peng et al., 2018; Zhao et al., 2019; Hu et al., 2020; Li et al., 2021; Xu et al., 2021; Li et al., 2022; Liu et al., 2022; Chen et al., 2023; Li et al., 2023; Peng et al., 2023; Shen et al., 2023). Modelling methods require drill hole data to validate the model, but due to the scarcity of ground stations on the QTP, these modelling studies lack sufficient validation (Li et al., 2012). The spatial characteristics of the ALT are generally studied on the basis of limited stations or simulations by extending the model to the entire QTP (Qin et al., 2017). For example, scientists have constructed permafrost distribution maps for different periods on the QTP, the resolution of these maps continues to increase, and the resolution of the latest maps of the spatial distribution of permafrost and ALT reaches 1 km (Zou et al., 2017; Ran et al., 2021; Cao et al., 2023; Shen et al., 2023).

Warming is significantly dependent on the altitude over the QTP, so the ALT has significant spatial variability and obvious distribution characteristics of the climatic zone (You et al., 2022). Solar radiation that is mainly manifested by temperature and precipitation have the greatest influence on ALT changes, as do elevation, longitude, latitude, the normalized difference vegetation index (NDVI), snow depth, and other factors (Karjalainen et al., 2019; Wang et al., 2020; Wang et al., 2021; Xu and Wu 2021). An increase in precipitation also leads to an increase in soil moisture on the QTP, and the cooling effect of precipitation can slow the warming rate and maintain the active layer at a relatively low temperature (Zhang et al., 2021; Ji et al., 2022). There are also differences in the ALT among different land use types; the mean ALT is approximately 1.5 m in the alpine meadow region and approximately 3 m in the cold desert area of the QTP (Wang et al., 2018). High vegetation cover reduces the effect of heat cycling on permafrost and can delay melting and freezing at a given depth (Wang et al., 2010). The process of energy transport in the soil, which often takes a long time, such as up to 10 months from the surface down to 320 cm, also has an impact on the ALT (Li et al., 2021). The ALT increases as the latitude increases, but the rate of increase gradually weakens, and it decreases with increasing altitude on the QTP (Cao et al., 2017). The ALT was 230 cm from 1990 to 2015 on the QTP, and it significantly increased at nearly all stations (Luo et al., 2016). The ALT thickening rate during 1969–2018 was 0.009 m/a on the QTP (Li et al., 2022). The average ALT increased from 2.68±0.52 m in 1901 to 2.87±0.46 m in 2020 in the "Three River" source region of the QTP (Chen et al., 2023). The ALT increases more significantly at low latitudes and high altitudes on the QTP (Luo et al., 2020; Shen et al., 2023).

Previous studies are limited by the uneven distribution of observation stations and the applicability of models or the inability to fully reflect the ability of soil temperature characterization at different depths when quantifying permafrost and the ALT on the QTP, and the results are also very uncertain. To overcome these limitations, the objective of this paper is to use the soil zero-degree layer as an index to evaluate the change in the ALT and to evaluate the possible changes in the spatial scale and time series of the soil freezing/melting capacity in the historical period and the future projected period of the QTP. Specifically, we calculated the soil zero-degree layer based on the interpolation of multilayer ground temperature data from

https://doi.org/10.5194/egusphere-2024-1169
Preprint. Discussion started: 13 May 2024

ground meteorological observation stations and different Coupled Model Intercomparison Project Phase 6 (CMIP6) global climate models (GCMs).

2 Data and Methods

2.1 Research Domain

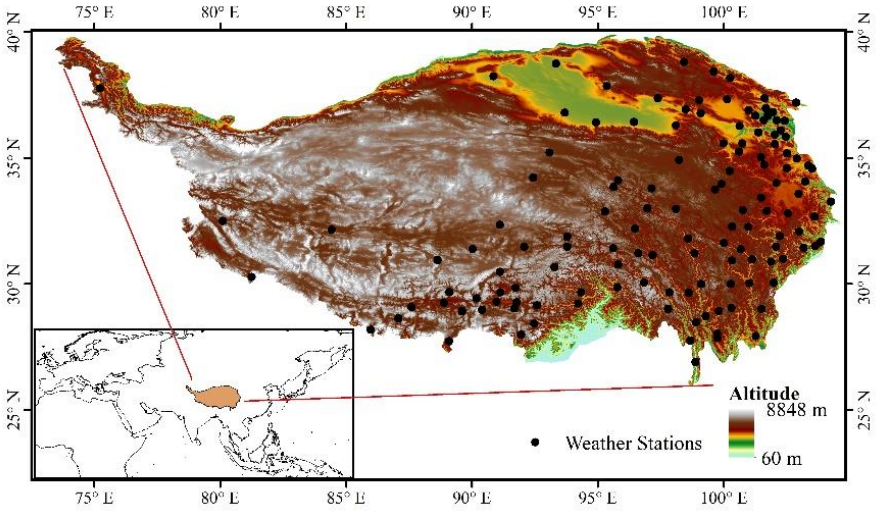

Figure 1: Topography map and locations of the 133 weather stations of the QTP

The Qinghai–Tibet Plateau (QTP) is located between 25 °-39 °N and 70 °-106 °E, and its total area is approximately 2.5×10^6 km^2, with an average altitude greater than 4,000 metres; it is known as the "roof of the world" or "third pole" (Fig. 1) (Deng et al., 2017). The QTP has one of the largest areas of permanent ice and snow in the mid-latitudes, and the Yangtze, Yellow and Brahmaputra Rivers all originate on the QTP and exhibit substantial glaciers, alpine lakes, and swamps (Yao et al., 2012; Lu et al., 2017). The temperatures exceed 15 ℃ in July but are less than -10 ℃ in January, and the average annual precipitation is approximately 450 mm, which is mostly concentrated from June to September, with precipitation decreasing from 2000 mm in the southeast to 50 mm in the northwest QTP (Yao et al., 2012; Lu et al., 2017; Zhao et al., 2019). Therefore, topographic, geomorphic and meteorological factors have jointly shaped the regional distribution characteristics of the southeastern region, which has a warm and humid climate, and the northwestern region, which has a cold and dry climate, on the QTP. The permafrost of the QTP is the highest and largest in area in the low and middle latitudes on Earth, accounting for more than half of the total area of the plateau; other areas contain seasonally frozen soil (Lu et al., 2017).

https://doi.org/10.5194/egusphere-2024-1169
Preprint. Discussion started: 13 May 2024

2.2 Data

2.2.1 Observed soil temperature

In this study, daily and monthly soil temperature data from 133 national meteorological stations on the QTP from 1961 to 2022 were measured at depths of 5 cm, 10 cm, 15 cm, 20 cm, 40 cm, 80 cm, 160 cm and 320 cm. The spatial distribution of the meteorological stations is shown in Fig. 1. The data included the longitude, latitude, and altitude of the meteorological stations and the near-surface temperature from 1961 to 2003, and the soil temperatures at depths of 0 cm, 5 cm, 10 cm, 15 cm, 20 cm and 40 cm were measured four times each day at 2:00, 8:00, 14:00 and 20:00 (BT). Soil temperatures at depths of 80 cm, 160 cm and 320 cm were measured once a day at 14:00 (BT). From 2004 to 2022, the soil temperature of each layer was measured 24 times per day (once each hour). For convenience of comparison, the average results of the soil temperature data of each layer are reported to 2 decimal places. The observed soil temperature data were obtained from the National Information Center of the China Meteorological Administration.

2.2.2 Soil temperature from GCMs

The monthly soil temperature data were obtained from 29 selected CMIP6 global climate models (GCMs) (https://esgf-node.llnl.gov/search/cmip6/). Table S1 shows the basic information of each model. As shown in Table S1, the maximum depths of the geothermal data of 29 CMIP6 models range from 1.945 m to 65.562 m, and the number of soil layers ranges from 3 to 25 in different models. Historical simulations of the 29 GCMs used for the horizontal spatial resolution of the model cover 1850-2014, and future climate projections cover 2015-2100 (O'Neill et al., 2016; Gidden et al., 2019). Among the latest shared socioeconomic pathways and representative concentration pathways (SSPs) of the CMIP6 models, the four typical scenarios, SSP1-2.6, SSP2-4.5, SSP3-7.0 and SSP5-8.5, represent the low-forcing scenario, medium-forcing scenario, medium-to-high-forcing scenario and high-forcing scenario, respectively. Due to the different resolutions of GCMs, to facilitate comparisons between each model and the multi-model ensemble average, the bilinear interpolation method was used to interpolate/extrapolate each model into a 0.5 °×0.5 ° longitude and latitude grid. In this study, the period from 1995 to 2014 was used as the reference period.

2.3 Method

2.3.1 Soil zero degree layer

For the soil temperature data of the meteorological stations, the bilinear extrapolation method was used to calculate the depth value of the soil temperature of 0 ℃ for each month in the vertical direction. The monthly soil temperature data from the CMIP6 GCMs were used to calculate the soil zero-degree soil layer depth in the vertical direction for each grid point.

https://doi.org/10.5194/egusphere-2024-1169
Preprint. Discussion started: 13 May 2024

2.3.2 Definition of global warming level of 1.5-5.0℃

The near-surface temperature warming thresholds selected in this study are calculated relative to the preindustrial temperature. We compare four typical scenarios in 29 selected CMIP6 GCMs for the historical period (1850-2014) and the future SSP1-2.6, SSP2-4.5, SSP3-7.0, and SSP5-8.5 with the average near-surface air temperature data for the preindustrial period (1850-1900). Based on the addition of the 20-year sliding average of the global mean near-surface air temperature to the preindustrial average for 29 models and four SSP scenarios, the annual means of the increases in the global mean air temperature reach the thresholds of 1.5 ℃, 2.0 ℃, 2.5 ℃, 3.0 ℃, 3.5 ℃, 4.0 ℃, 4.5 ℃ and 5.0 ℃ (Table S2). The use of a 20-year running average for each specific warming threshold, which is a time-sampling method used in many previous papers, also provides credible results (Jiang et al., 2020; Miao et al., 2020; Gao et al., 2021; Mondal et al., 2021; Huang et al., 2022). Some models and scenarios fail to reach specific warming threshold targets, suggesting that these models or scenarios do not account for a specific warming level in the future projected period (2015-2100) but that the threshold may have already occurred in the simulated historical period. For example, the EC-Earth3-Veg model cannot calculate the period in which the 1.5℃ warming threshold is reached in its projected period (2015-2100) under all SSP scenarios. In some low-forcing scenarios, higher warming thresholds, such as the 2.5 ℃, 3.0 ℃, 3.5 ℃, 4.0 ℃, 4.5 ℃ and 5.0 ℃ thresholds for the future projected period EC-Earth3-Veg model under the SSP1-2.6 scenario, cannot be achieved.

Taking one model under one SSP as the data set, the numbers of data sets under the different global warming levels are listed in Table 1. At a global warming level of 1.5℃, there are 81 data sets, while for a global warming level of 2.0 ℃, there are 97 data sets; then, the number of data sets decreases with global warming levels, and there are only 18 data sets for the global warming level of 5.0 ℃.

Table 1 The number of data sets at different global warming levels

Global warming levels	Number of models×SSPs (Total：29×4=116)
1.5℃	81
2.0℃	97
2.5℃	86
3.0℃	70
3.5℃	56
4.0℃	38
4.5℃	23
5.0℃	18

https://doi.org/10.5194/egusphere-2024-1169
Preprint. Discussion started: 13 May 2024

3 Result

3.1 Model performance evaluation

To investigate the simulation performance of the CMIP6 model for the QTP soil temperature in the vertical direction, we compared the data from 9 weather stations in Gangcha, Golmud, Henan, Lenghu, Mangya, Kangding, Pulan, Menyuan, and Hezuo. The soil temperatures of each layer from the model results of the grid point where the meteorological station is located were extracted and compared with the soil temperature data of depths of 0.05-3.2 m for each layer observed by the meteorological station. The results for July are shown in Fig. 2. Since the maximum depth of the observed data is only 3.2 m, the depth of the soil temperature profile shown in the figure is selected to be within 4 m. Fig. 2 shows that the soil temperature observed in the vertical direction decreases with increasing depth; the closer to the surface, the higher the soil temperature is, and the trends at the nine sites are consistent. The result of the GCMs is that the soil temperature decreases with increasing depth, but the rate of soil temperature decrease is different. This indicates that the observed soil temperature is consistent with the GCM simulation results in the vertical direction. Notably, most of the simulated soil temperatures of the GCMs are lower than the observed temperatures, which are almost the same for every depth, indicating that the soil temperatures simulated by the models are generally low. In other words, there is a deviation towards colder in the soil temperature simulated by the GCM models.

https://doi.org/10.5194/egusphere-2024-1169
Preprint. Discussion started: 13 May 2024

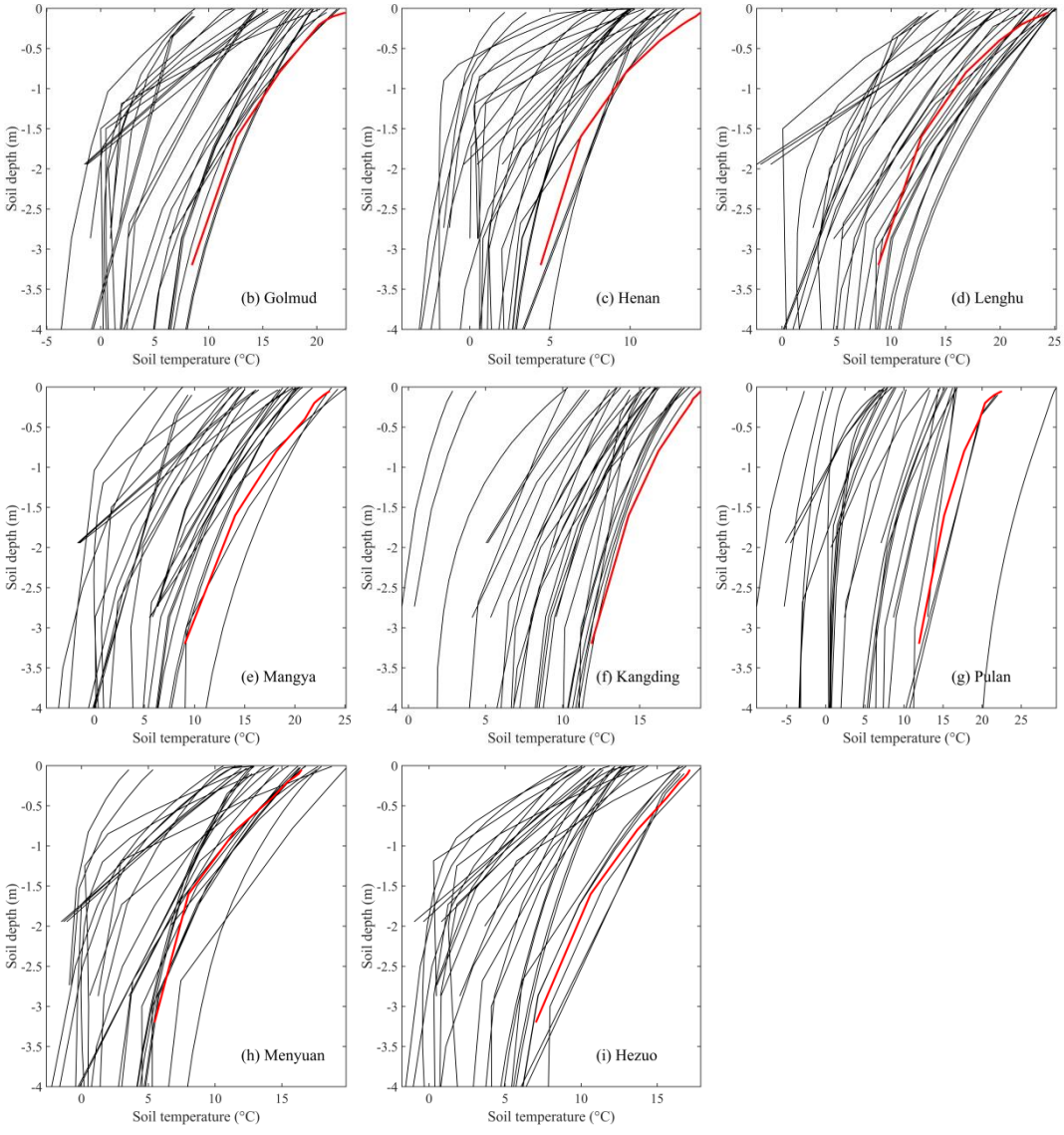

Figure 2: Profiles for the observed (red lines) and GCMs simulated (black lines) soil temperature of selected meteorological stations in July in the QTP region.

https://doi.org/10.5194/egusphere-2024-1169
Preprint. Discussion started: 13 May 2024

3.2 Changes of ALT in observed period

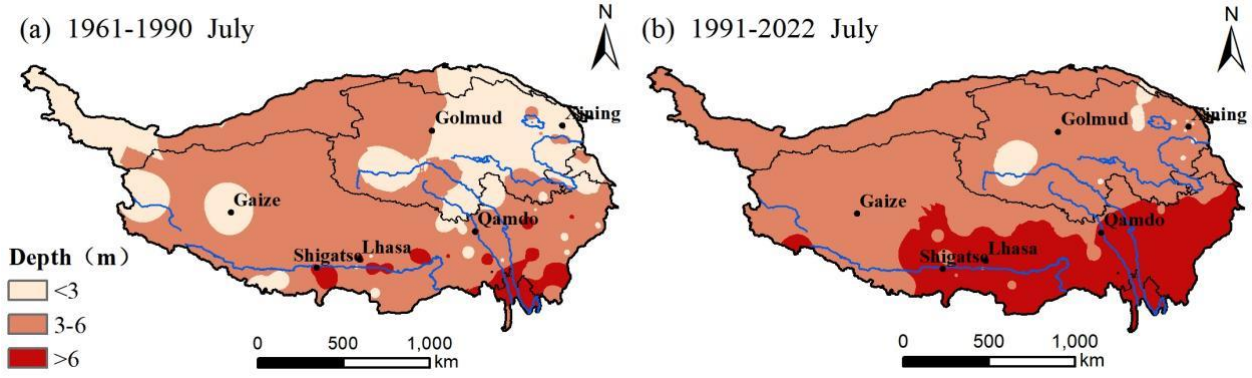

Figure 3: Spatial patterns of ALT in July during (a) 1961-1990 and (b)1991-2022.

Since most areas of the QTP are frozen in winter, it is not suitable to investigate the changes in the soil layer at 0 ℃, so we chose July as a typical summer month for analysis. As shown in Fig. 3, we analysed the interdecadal variation in the ALT in July during 1961-1990 and 1991-2022 on the QTP. Fig. 3(a) shows that during 1961-1990, the ALTs on the QTP were approximately 1.10-15.91 m, with an average of 3.75 m. The ALTs were approximately 1.72-13.53 m, with an average of 5.77 m, during 1991-2022. The average ALTs increased by 53.9% from 1991-2022 compared to those from 1961-1990.

In terms of spatial distribution, the areas with ALTs less than 3 m in 1961-1990 composed approximately 30% of the QTP area and were mainly distributed in the western Pamir Plateau, near Gaize, north of Qamdo in the northeast and east of Golmud over the QTP. Areas with ALTs greater than 6 m accounted for only 4.3% of the QTP area and were scattered in the southeastern QTP area, i.e., east and south of Shigatse and Lhasa. In the other 65.8% of the area, the ALTs were 3-6 m. As global warming progresses, the QTP is also warming (Chen et al., 2022). From 1991 to 2022, the spatial distribution in the ALT in the QTP soil changed significantly. ALTs less than 3 m composed approximately 2.5% of the QTP area and were scattered in the central and northeastern parts of the QTP. ALTs deeper than 6 m composed approximately 26.4% of the QTP area and were mainly distributed in the southeastern part of the QTP near and south of the Shigatse-Lassa-Qamdo line. ALTs in the other 71.1% of the QTP area were 3-6 m. Compared with the period of 1961-1990, the changes in the areas where the ALTs were less than 3 m, 3-6 m and greater than 6 m over the QTP during 1991-2022 were -91.8%, 8.1% and 519.5%, respectively.

3.3 Project changes in soil zero layer

https://doi.org/10.5194/egusphere-2024-1169
Preprint. Discussion started: 13 May 2024

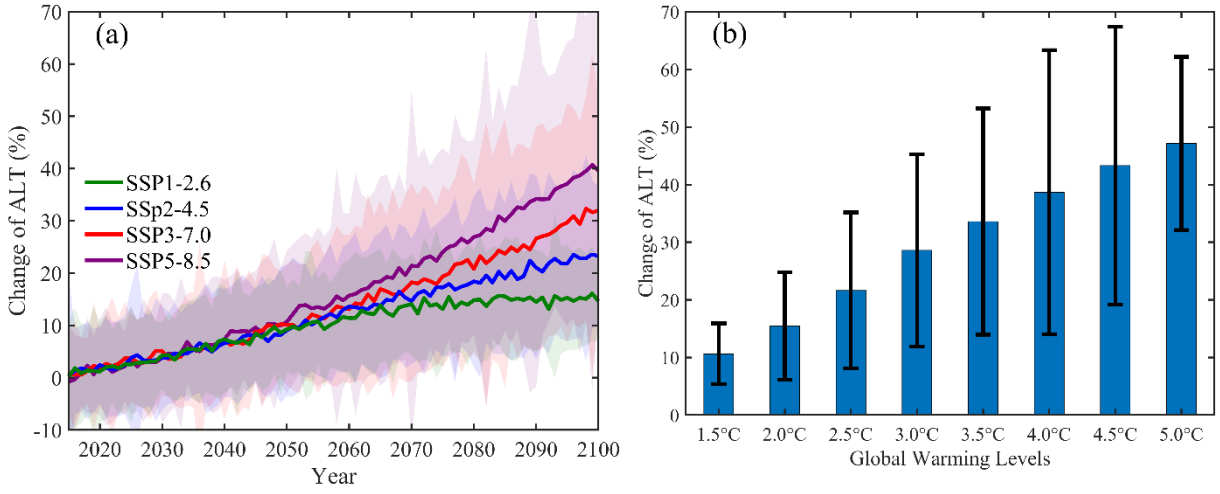

Figure 4: The changes of regionally average ALT under the different global warming levels over the Qinghai-Tibetan Plateau (QTP) projected by 29 CMIP6 models. (a) Time series of multi-model mean under four SSPs, (b) Under 1.5℃, 2.0℃, 2.5℃, 3.0℃, 3.5℃, 4.0℃, 4.5℃ and 5.0℃ warming targets relative to the reference period (1995-2014). Note: a) Different colour shading represents plus/minus one standard deviation among the models from their ensemble mean; b) The straight black lines indicate plus/minus one standard deviation of multiple GCMs under different global warming levels.

The ALT is an important index for studying changes in frozen soil on the QTP. A time series of the differences in the ALT changes from 2015–2100 relative to the reference period (1995–2014) demonstrate that the four SSPs exhibit different changes of varying magnitudes (Fig. 4(a)). Under the SSP1-2.6 scenario, the change in the ALT relative to that in the reference period continues to increase from 2015 to 2065 and then fluctuates at approximately 15%. Under SSP2-4.5, SSP3-7.0 and SSP5-8.5, the change in the ALT will continue to increase throughout the future project period, and the increase will be more rapid with increasing radiative forcing. Under SSP5-8.5, the greatest projected increase of 39.6% will occur by the end of the 21st century across the QTP.

The changes in the regional average ALTs under 1.5 ℃, 2.0 ℃, 2.5 ℃, 3.0 ℃, 3.5 ℃, 4.0 ℃, 4.5 ℃ and 5.0 ℃ global warming levels relative to 1995-2014 are shown in Fig. 4(b). As shown in Fig. 4(b), under the threshold of global warming levels of 1.5-5.0 ℃ in the future, the regional average ALT of the QTP will increase consistently compared with that in the reference period, and the change in the ALT will gradually increase. When global warming level reach the 1.5 ℃, 2.0 ℃, 2.5 ℃, 3.0 ℃, 3.5 ℃, 4.0 ℃, 4.5 ℃ and 5.0 ℃ thresholds, the average ALTs in the QTP region will increase by 10.6%, 15.4%, 21.6%, 28.6%, 33.6%, 38.7%, 43.3% and 47.1%, respectively. This means that for each 0.5 ℃ temperature increase, the ALTs of the QTP will increase by 5.4%. The correlation coefficient R^2 between the ALT and the temperature increase is 0.9938. Moreover, there are substantial regional differences.

.

https://doi.org/10.5194/egusphere-2024-1169
Preprint. Discussion started: 13 May 2024

3.4 Spatial variations in the changes of ALT

In terms of spatial distribution, the changes in the ALT under eight different global warming levels (1.5 ℃, 2.0 ℃, 2.5 ℃, 3.0 ℃, 3.5 ℃, 4.0 ℃, 4.5 ℃ and 5.0 ℃) relative to the reference period (1995-2014) are shown in Fig. 5. Overall, the ALT is projected to increase substantially across the entire QTP under all global warming levels, and the greater the temperature increase is, the greater the increase in depth. Under temperature increases of 1.5 ℃, 2.0 ℃, 2.5 ℃, 3.0 ℃, 3.5 ℃, 4.0 ℃, 4.5 ℃ and 5.0 ℃, the coverage areas with ALT increases less than 20% are approximately 54.9%, 36.4%, 26.6%, 16.4%, 10.9%, 5.3% and 2.4%, respectively. This means that the coverage area where the ALT decreases less than 20% decreases with increasing temperatures, with values that change from 1,424,735 km^2 at 1.5 ℃ to 13,682 km^2 at 5.0 ℃ warming thresholds. The proportions of the total QTP area where the ALT increase by 20%-50% are 43.2%, 52.0%, 43.5%, 38.8%, 39.2%, 41.8%, 41.0% and 36.5%, respectively. The depths that increase by 50%-100% are 1.9%, 11.5%, 29.0%, 38.0%, 41.6%, 43.9%, 46.0% and 47.5%, respectively. This also means that the area increases from 48,174 km^2 to 1,232,073 km^2. The percentages of areas with ALT increases >100% are 0%, 0.1%, 0.9%, 6.8%, 8.3%, 9.0%, 10.5% and 15.5% at 1.5 ℃, 2.0 ℃, 2.5 ℃, 3.0 ℃, 3.5 ℃, 4.0 ℃, 4.5 ℃ and 5.0 ℃, respectively. Compared to the area with a small increase in the ALT, the area with a greater than 100% increase reflects a sharp increase from 0 at 1.5 ℃ to 401,433 km^2 at 5.0 ℃.

Furthermore, at the same global warming level, relatively small increases in the ALT are distributed in the northeastern, eastern and southeastern regions of the QTP, such as Golmud, Xining, and Shigatse. The areas with a large depth increase are concentrated in the western region, such as the areas north and west of Gaize, which is also the area with a concentrated distribution of permafrost. In other words, the ALT increases more rapidly in the central and western regions of the QTP. Overall, the magnitude of the ALT is projected to increase with warming climate conditions across the QTP.

With respect to the rate of change in the ALT under 0.5 ℃ of warming, the ALT increases for almost the entire QTP during the projected period. In the areas south of Shigatse, Lhasa and Qamdo and north of Golmud, the rate of change is less than 5% per 0.5 ℃, and the coverage area is approximately 45.0% of the QTP. In the areas north and west of Gaize, the rate of change is more than 10% every 0.5 ℃, and the coverage area is approximately 39.5% of the QTP. Other areas of the QTP change at rates of 5-10% per 0.5 ℃, covering an area of approximately 15.2% of the QTP (Fig. 5(i)).

In this study, areas where the rate of ALT increase was not severe (< 50%) in the coverage area were dominant at global warming levels of 1.5 ℃, 2.0 ℃, 2.5 ℃, 3.0 ℃ and 3.5 ℃ (Fig. 5a-e). When the temperature increases to 4.0 ℃, 4.5 ℃ and 5.0 ℃, the soil depth increases more sharply (>50%) in the region (Fig. 5f-h).

https://doi.org/10.5194/egusphere-2024-1169
Preprint. Discussion started: 13 May 2024

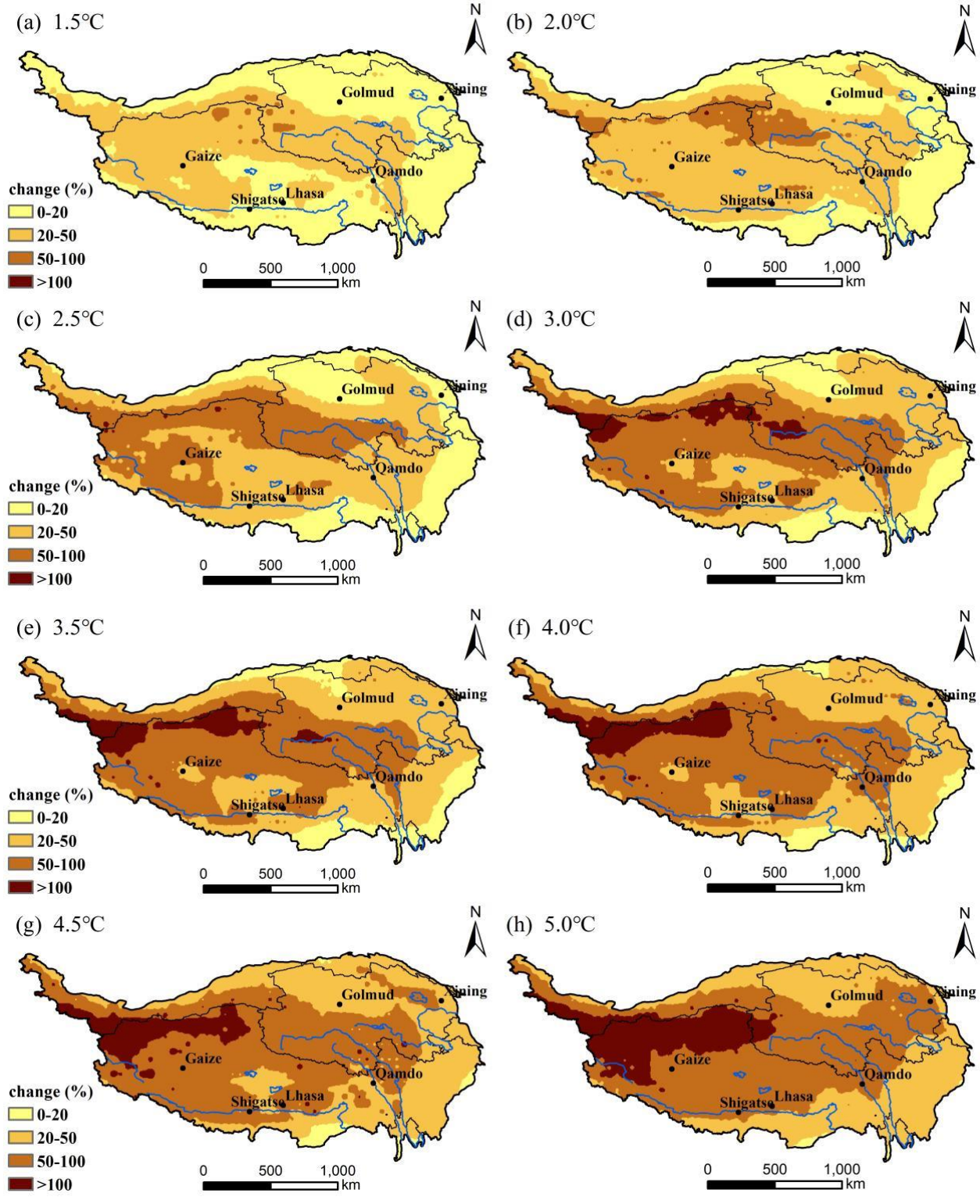

https://doi.org/10.5194/egusphere-2024-1169
Preprint. Discussion started: 13 May 2024

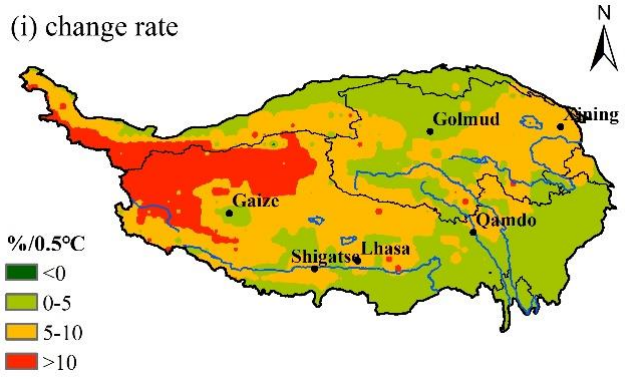

Figure 5: The spatial distribution of ALT changes over the QTP area at (a)1.5℃, (b) 2.0℃, (c)2.5℃, (d)3.0℃, (e)3.5℃, (f) 4.0℃, (g)4.5℃ and (h) 5.0℃ global warming levels and (i) change rate per 0.5℃ relative to the reference period (1995-2014).

4 Discussion

Although 133 meteorological stations were used to analyse the change in the ALT across the QTP, this observation network is still low in the density of stations due to the vast area and complex topography of the QTP, which limits our ability to assess ALT changes in remote areas of the plateau. Our observed results showed that the ALT increases from the first period (1961-1990) to the second period (1991-2022), which indicates a persistent and rapid warming trend over the QTP. While these findings can enhance our understanding of the effects of changing air temperature conditions on soil freezing capacity on the QTP, sparse observations in the plateau region introduce uncertainties and limitations to our understanding. However, our purpose is to analyse the spatial distribution and trend of ALT variation over a large region rather than to determine accurate values.

The results of the ALT obtained by the simple linear extrapolation method also have uncertainties. For example, we selected only the soil temperature data from the warmest summer (July) to determine the change in ALT, while in winter (January), the linear extrapolation method could not be used, and the results were extrapolated to the air. The ALT obtained by the linear extrapolation method is much greater than the maximum soil temperature at most meteorological stations and at some grid points in the CMIP6 model data. For example, the observed maximum depth of soil temperature is 3.2 m, but the calculated average effective data of the ALT of the regional average across the QTP during 1961-1990 is 3.75 m, the maximum value is 15.9 m, and the minimum value is only 1.10 m. The spatial distribution is influenced by climate characteristics and physical mechanisms, but it also inevitably introduces some uncertainties. Moreover, for the results of the 29 GCMs, the regional average values of ALT greatly differ among the models. For example, during the reference period (1995-2014), the minimum ALT calculated from model data was only 1.3 m (GISS-E2-1-H), while the maximum was 43.8 m (NorESM2-LM). Among these values, the ALTs calculated by 15 GCMs are smaller or similar to the observed ALTs, while those of the other 14 models are larger than the observed ALTs.

https://doi.org/10.5194/egusphere-2024-1169
Preprint. Discussion started: 13 May 2024

The effects of global warming on QTP permafrost degradation, seasonal permafrost and ALT changes can be better analysed by studying the changes in the soil zero-degree layer. In contrast to the new frozen soil map, this study revealed that permafrost degradation accelerates more rapidly with increasing temperatures in the western permafrost area of the QTP (Cao et al., 2023). In this study, without bias correction of the soil temperature data from CMIP6, the ALTs of 15 models, namely, GISS-E2-1-H, GISS-E2-1-G, EC-Earth3, EC-Earth3-VEG, EC-Earth3-VEG-LR, and BCC-CSM2-MR, were obtained. The results of the UKESM1-0-LL, ACCESS-ESM1-5, ACCESS-CM2, GFDL-ESM4, CNRM-CM6-1, CanESM5, CanESM5-1, CNRM-ESM2-1 and MRI-ESM2-0 models are close to the observed values.

In addition, CMIP6 model data with resolutions ranging from tens to hundreds of kilometres cannot be finely characterized when analysing spatial heterogeneity and local changes. The ability of each CMIP6 model to simulate the soil temperature depth is different, the number of soil temperature layers is very different, and the depth of the soil temperature in each layer is also inconsistent, all of which have an impact on the results of the ALT.

This study represents a step towards understanding the changes in the soil temperature structure of the QTP in the context of global temperature increases. The results of this study provide a possibility for predicting changes in permafrost and the active layer on the QTP in the 21st century.

Overall, the insights from this study on the changes in the ALT have wider applicability for analysing permafrost degradation in a warming climate. In this paper, providing an accurate result is not our aim; instead, we attempt to use the soil zero-degree layer as a reasonable indicator that reflects permafrost and the ALT over the QTP from a vertical perspective. When considering soil temperature, factors such as the water/ice distribution profile of the soil, soil composition types, soil heat flux transfer, ground surface vegetation index, and land use types are considered to obtain results at higher precision and spatial resolution in the future.

5 Conclusions

In this study, we assessed future changes in the soil zero-degree layer under different temperature increases on the Qinghai–Tibet Plateau. This study provided a snapshot of the possible effects of soil freezing depth changes caused by rising soil temperature on permafrost and ALT changes. The following conclusions can be drawn:

(1) The soil temperature simulated by the CMIP6 GCMs in July on the QTP in the vertical direction is consistent with the observed trend of soil temperature with depth, and both decrease with increasing soil depth. At the same time, the soil temperature of each layer of the GCMs exhibited cold deviations compared with the observed values.

(2) The average ALT on the Qinghai–Tibet Plateau was approximately 3.75 m (range of 1.10~15.91 m) from 1961-1990 and increased to 5.77 m (range of 1.72~13.53 m) from 1991 to 2022, an increase of 53.9%. The observed ALTs were >6 m in the southeastern QTP area, such as east and south of Shigatse and Lhasa, where the ALT was <3 m in the western Pamir Plateau, near Gaize, north of Qamdo in the northeast and east of Golmud, and other central and northern regions, where it was 3-6 m.

https://doi.org/10.5194/egusphere-2024-1169
Preprint. Discussion started: 13 May 2024

(3) In the project period (2015-2100), under the SSP1-2.6, the increase in the ALT will continue to increase compared with that in the reference period (1995-2014) before 2065 and then fluctuate at approximately 15%. Under the SSP2-4.5, SSP3-7.0 and SSP5-8.5 scenarios, the ALT will continue to increase, and the greater the radiative forcing level is, the faster it will increase. By the end of the 21st century, the ALT of the entire QTP will experience a maximum projected increase of 39.6% under the SSP5-8.5 scenario.

(4) When the global warming levels reach the thresholds of 1.5℃-5.0℃ in the future, the regional average ALT over the QTP will increase by 10.6%-47.1%, which means that it will increase by 5.4% per 0.5℃ increase.

(5) Under temperature increases of 1.5 ℃-5.0 ℃, the area with small changes (e.g., <20%) in the ALT will decrease with temperature, from 1,424,735 km^2 to 13,682 km^2. The area with a 50-100% increase will change from 48,174 km^2 to 1,232,073 km^2. The area with a depth increase of >100% will change from 0 to 401,433 km^2. Under the same global warming level, the areas with a small increase in the ALT are distributed in the northeast, east and southeast regions of the QTP, and the areas with a large increase in depth are concentrated in the area with a concentrated distribution of permafrost in the western region.

Data availability. All CMIP6 model outputs [Dataset] are openly available from phase 6 of the Coupled Model Intercomparison Project (CMIP6) can be downloaded from https://esgf-data.dkrz.de/search/cmip6-dkrz/. The observation data of weather stations that support the findings of this study are not openly available due to restrictions of distributing the data and are available from the corresponding author upon reasonable request.

Authors Contributions. T. Jiang, J.L. Huang and Z.J. Li conceived the study. Z.J. Li and B.D. Su are performing analyses and drafting the paper. B.D. Su, J.L. Huang, R.H. Xu, C. Jing and Y. Gong calculated soil zero layer and analysed it from observation dataset. T. Jiang and P.H. Havea integrated innovative ideas and improved the complete research and manuscript. All authors discussed the results and edited the manuscript.

Competing interests. The authors declare that they have no conflict of interest.

References

Cao, B., Gruber, S., Zhang, T., Li, L., Peng, X., Kang, W., Zheng, L., Shao, W., and Guo, H.: Spatial variability of active layer thickness detected by ground-penetrating radar in the Qilian Mountains, Western China. Journal of Geophysical Research: Earth Surface, 122(3), 574–591. https://doi.org/10.1002/2016jf004018, 2017.

Cao, Z., Nan, Z., Hu, J., Chen, Y., and Zhang, Y.: A new 2010 permafrost distribution map over the Qinghai–Tibet Plateau based on subregion survey maps: a benchmark for regional permafrost modeling. Earth System Science Data, 15(9), 3905-3930. https://doi.org/10.5194/essd-15-3905-2023, 2023.

https://doi.org/10.5194/egusphere-2024-1169
Preprint. Discussion started: 13 May 2024

Chen, F., Luo, D., Gao, Y., and Lei, W.: Decadal expansion and contraction of permafrost in the Three-River Source Region, Qinghai-Tibet Plateau (1901-2020). Advances in Climate Change Research, 14(2), 226-236. https://doi.org/10.1016/j.accre.2023.04.003, 2023.

Chen, R., Li, H., Wang, X., Gou, X., Yang, M., and Wan, G.: Surface air temperature changes over the Tibetan Plateau: Historical evaluation and future projection based on CMIP6 models. Geoscience Frontiers, 13(6), 101452. https://doi.org/10.1016/j.gsf.2022.101452, 2022.

Cheng, G., and Wu, T.: Responses of permafrost to climate change and their environmental significance, Qinghai-Tibet Plateau. Journal of Geophysical Research: Earth Surface, 112(F2). https://doi.org/10.1029/2006JF000631, 2007.

Cheng, G., Zhao, L., Li, R., Wu, X., Sheng, Y., Hu, G., Hu, G., Zou, D., Jin, H., Li, X., and Wu, Q.: Characteristic, changes and impacts of permafrost on Qinghai-Tibet Plateau. Chinese Science Bulletin, 64(27), 2783–2795. https://doi.org/10.1360/tb-2019-0191, 2019.

Deng, H., Pepin, N.C., and Chen, Y.: Changes of snowfall under warming in the Tibetan Plateau. J. Geophys. Res. Atmos. 122 (14), 7323–7341. https://doi.org/10.1002/2017JD026524, 2017.

Ding, J., Chen, L., Ji, C., Hugelius, G., Li, Y., Liu, L., Qin, S., Zhang, B., Yang, G., Li, F., Fang, K., Chen, Y., Peng, Y., Zhao, X., He, H., Smith, P., Fang, J., and Yang, Y.: Decadal soil carbon accumulation across Tibetan permafrost regions. Nature Geosci 10, 420–424. https://doi.org/10.1038/ngeo2945, 2017.

Ding, Y., Zhang, S., Zhao, L., Li, Z., and Kang, S.: Global warming weakening the inherent stability of glaciers and permafrost. Science Bulletin, 64(4), 245-253. https://doi.org/10.1016/j.scib.2018.12.028, 2019.

Gao, M., Kim, S.J., Yang, J., Liu, J., Jiang, T., Su, B., Wang, Y., and Huang, J.: Historical fidelity and future change of Amundsen Sea Low under 1.5℃-4℃ global warming in CMIP6. Atmos. Res. 255, 105533. https://doi.org/10.1016/j.atmosres.2021.105533, 2021.

Gao, T., Zhang, Y., Kang, S., Abbott, B. W., Wang, X., Zhang, T., Yi, S., and Gustafsson, Ö.: Accelerating permafrost collapse on the eastern Tibetan Plateau. Environmental Research Letters, 16(5), 054023. https://doi.org/10.1088/1748-9326/abf7f0, 2021.

Gidden, M.J., Riahi, K., Smith, S.J., Fujimori, S., Luderer, G., Kriegler, E., Vuuren, D.P.V., van den Berg, M., Feng, L., Klein, D., Calvin, K., Doelman, J.C., Frank, S., Fricko, O., Harmsen, M., Hasegawa, T., Havlik, P., Hilaire, J., Hoesly, R., Horing, J., Popp, A., Takahashi, K.: Global emissions pathways under different socioeconomic scenarios for use in CMIP6: A dataset of harmonized emissions trajectories through the end of the century. Geosci. Model Dev. 12, 1443–1475. https://doi.org/10.5194/gmd-12-1443-2019, 2019.

Guo, D., and Wang, H.: Simulation of permafrost and seasonally frozen ground conditions on the Tibetan Plateau, 1981–2010. Journal of Geophysical Research: Atmospheres, 118(11), 5216-5230. https://doi.org/10.1002/jgrd.50457, 2013.

Guo, D., and Wang, H.: Permafrost degradation and associated ground settlement estimation under 2℃ global warming. Climate Dynamics 49, 2569–2583. https://doi.org/10.1007/s00382-016-3469-9, 2017.

https://doi.org/10.5194/egusphere-2024-1169
Preprint. Discussion started: 13 May 2024

Guo, D., Wang, H., and Li, D.: A projection of permafrost degradation on the Tibetan Plateau during the 21st century. Journal of Geophysical Research: Atmospheres, 117(D5). https://doi.org/10.1029/2011JD016545, 2012.

Hu, G., Zhao, L., Li, R., Wu, X., Wu, T., Xie, C., Zhu, X., and Hao, J.: Estimation of ground temperatures in permafrost regions of the Qinghai-Tibetan Plateau from climatic variables. Theoretical and Applied Climatology, 140, 1081-1091. https://doi.org/10.1007/s00704-020-03135-1, 2020.

Huang, J., Mondal, S. K., Zhai, J., Fischer, T., Wang, Y., Su, B.,Wang, G., Gao, M., Jiang, S., Tao, H., Lin, Q., and Jiang, T.: Intensity-area-duration-based drought analysis under 1.5 C–4.0 C warming using CMIP6 over a climate hotspot in South Asia. Journal of Cleaner Production, 345, 131106. https://doi.org/10.1016/j.jclepro.2022.131106, 2022.

Ji, F., Fan, L., Kuang, X., Li, X., Cao, B., Cheng, G.,Yang Y., and Zheng, C.: How does soil water content influence permafrost evolution on the Qinghai-Tibet Plateau under climate warming?. Environmental Research Letters, 17(6), 064012. https://doi.org/10.1088/1748-9326/ac6c9a, 2022.

Karjalainen, O., Luoto, M., Aalto, J., and Hjort, J.: New insights into the environmental factors controlling the ground thermal regime across the Northern Hemisphere: a comparison between permafrost and non-permafrost areas. The Cryosphere, 13(2), 693-707. https://doi.org/10.5194/tc-13-693-2019, 2019.

Li, G., Zhang, M., Pei, W., Melnikov, A., Khristoforov, I., Li, R., and Yu, F.: Changes in permafrost extent and active layer thickness in the Northern Hemisphere from 1969 to 2018. Science of The Total Environment, 804, 150182. https://doi.org/10.1016/j.scitotenv.2021.150182, 2022.

Li, M., Ma, Z., Wu, P., Liu, J., Lv, M., Yang, Q., and Han, Y.: Ecological response to climate change across China from combined soil temperature and moisture changes. Earth and Space Science, 9, e2022EA002640. https://doi.org/10.1029/2022EA002640, 2022.

Li, R., Xie, J., Xie, Z., Gao, J., Jia, B., Qin, P., Wang L., Wang Y, Liu B., and Chen, S.: Simulated response of the active layer thickness of permafrost to climate change. Atmospheric and Oceanic Science Letters, 14(1), 100007. https://doi.org/10.1016/j.aosl.2020.100007, 2021.

Li, R., Zhang, M., Andreeva, V., Pei, W., Zhou, Y., Misailov, I., and Basharin, N.: Impact of climate warming on permafrost changes in the Qinghai-Tibet Plateau. Cold Regions Science and Technology, 205, 103692. https://doi.org/10.1016/j.coldregions.2022.103692, 2023.

Li, R., Zhao, L., Ding, Y., Wu, T., Xiao, Y., Du, E., Liu, G., and Qiao, Y.: Temporal and spatial variations of the active layer along the Qinghai-Tibet Highway in a permafrost region. Chinese Science Bulletin, 57, 4609-4616. https://doi.org/10.1007/s11434-012-5323-8, 2012.

Li, Y., Zhang, C., Li, Z., Yang, L., Jin, X., and Gao, X.: Analysis on the temporal and spatial characteristics of the shallow soil temperature of the Qinghai-Tibet Plateau. Scientific Reports, 12(1), 19746. https://doi.org/10.1038/s41598-022-23548-4, 2022.

Liu, Q., Niu, J., Lu, P., Dong, F., Zhou, F., Meng, X., Xu, W., Shan Li., and Hu, B. X.: Interannual and seasonal variations of permafrost thaw depth on the Qinghai-Tibetan plateau: A comparative study using long short-term memory, convolutional

https://doi.org/10.5194/egusphere-2024-1169
Preprint. Discussion started: 13 May 2024

neural networks, and random forest. Science of The Total Environment, 838, 155886. http://dx.doi.org/10.1016/j.scitotenv.2022.155886, 2022.

Lu, Q., Zhao, D., and Wu, S.: Simulated responses of permafrost distribution to climate change on the Qinghai–Tibet Plateau. Sci Rep 7, 3845. https://doi.org/10.1038/s41598-017-04140-7, 2017.

Luo, D., Wu, Q., Jin, H., Marchenko, S. S., Lü, L., and Gao, S.: Recent changes in the active layer thickness across the northern hemisphere. Environmental Earth Sciences, 75(7), 555. https://doi.org/10.1007/s12665-015-5229-2, 2016.

Luo, S., Wang, J., Pomeroy, J. W., and Lyu, S.: Freeze–thaw changes of seasonally frozen ground on the Tibetan Plateau from 1960 to 2014. Journal of Climate, 33(21), 9427-9446. https://doi.org/10.1175/JCLI-D-19-0923.1, 2020.

Miao, L., Li, S., Zhang, F., Chen, T., Shan, Y., Zhang, Y.: Future drought in the dry lands of Asia under the 1.5 and 2.0℃ warming scenarios. Earth's Future 8, e2019EF001337. https://doi.org/10.1029/2019ef001337, 2020.

Mondal, S. K., Huang, J., Wang, Y., Su, B., Kundzewicz, Z.W., Jiang, S., Zhai, J., Chen, Z., Jing, C., and Jiang, T.: Changes in extreme precipitation across South Asia for each 0.5℃ of warming from 1.5℃ to 3.0℃ above pre-industrial levels. Atmos. Res. 266, 105961. https://doi.org/10.1016/j.atmosres.2021.105961, 2021.

O'Neill, B.C., Tebaldi, C., van Vuuren, D.P., Eyring, V., Friedlingstein, P., Hurtt, G., Knutti, R., Kriegler, E., Lamarque, J.-F., Lowe, J., Meehl, G.A., Moss, R., Riahi, K., Sanderson, B.M.: The scenario model intercomparison project (ScenarioMIP) for CMIP6. Geosci. Model Dev. 9, 3461–3482. https://doi.org/10.5194/gmd-9-3461-2016, 2016.

Pang, Q., Cheng, G., Li, S., and Zhang, W.: Active layer thickness calculation over the Qinghai–Tibet Plateau. Cold Regions Science and Technology, 57(1), 23-28. https://doi.org/10.1016/j.coldregions.2009.01.005, 2009.

Pang, Q., Zhao, L., Li, S., and Ding, Y.: Active layer thickness variations on the Qinghai-Tibet Plateau under the scenarios of climate change. Environ Earth Sci 66 (3): 849–857. https://doi.org/10.1007/s12665-011-1296-1, 2012.

Peng, X., Zhang, T., Frauenfeld, O. W., Kang, W., Luo, D., Cao, B., Su, H., Jin, H., and Wu, Q.: Spatiotemporal changes in active layer thickness under contemporary and projected climate in the Northern Hemisphere. Journal of Climate, 31(1), 251–266. https://doi.org/10.1175/jcli-d-16-0721.1, 2018.

Peng, X., Zhang, T., Frauenfeld, O. W., Mu, C., Wang, K., Wu, X., Guo, D., Luo, J., Hjort, J., Aalto, J., Karjalainen, O., and Luoto, M.: Active layer thickness and permafrost area projections for the 21st century. Earth's Future, 11, e2023EF003573. https://doi.org/10.1029/2023EF003573, 2023.

Qin, Y., Wu, T., Zhao, L., Wu, X., Li, R., Xie, C., Pang, Q., Liu, G., Zhu, X., and Hao, J.: Numerical modeling of the active layer thickness and permafrost thermal state across Qinghai-Tibetan Plateau. Journal Geophysical Research: Atmospheres, 122, 11,604–11,620. https://doi.org/10.1002/2017JD026858, 2017.

Ran, Y., Cheng, G., Dong, Y., Hjort, J., Lovecraft, A. L., Kang, S., Tan, M., and Li, X.: Permafrost degradation increases risk and large future costs of infrastructure on the Third Pole. Communications Earth & Environment, 3(1), 238. https://doi.org/10.1038/s43247-022-00568-6, 2022.

Ran, Y., Li, X., and Cheng, G.: Climate warming over the past half century has led to thermal degradation of permafrost on the Qinghai–Tibet Plateau. The Cryosphere, 12(2), 595-608. https://doi.org/10.5194/tc-12-595-2018, 2018.

https://doi.org/10.5194/egusphere-2024-1169
Preprint. Discussion started: 13 May 2024

Ran, Y., Li, X., Cheng, G., Nan, Z., Che, J., Sheng, Y., Wu, Q., Jin, H., Luo, D., Tang, Z., and Wu, X.: Mapping the permafrost stability on the Tibetan Plateau for 2005–2015. Sci. China Earth Sci. 64, 62–79. https://doi.org/10.1007/s11430-020-9685-3, 2021.

Shen, T., Jiang, P., Ju, Q., Yu, Z., Chen, X., Lin, H., and Zhang, Y.: Changes in permafrost spatial distribution and active layer thickness from 1980 to 2020 on the Tibet Plateau. Science of The Total Environment, 859, 160381. http://dx.doi.org/10.1016/j.scitotenv.2022.160381, 2023.

Wang, C., Dong, W., and Wei, Z.: Anomaly feature of seasonal frozen soil variations on the Qinghai-Tibet Plateau. Journal of Geographical Sciences, 12, 99-107. https://doi.org/10.1007/BF02837433, 2002.

Wang, C., Zhang, Z., Zhang, H., Zhang, B., Tang, Y., and Wu, Q.: Active layer thickness retrieval of Qinghai–Tibet permafrost using the TerraSAR-X InSAR technique. IEEE Journal of Selected Topics in Applied Earth Observations and Remote Sensing, 11(11), 4403-4413. https://ieeexplore.ieee.org/abstract/document/8526283, 2018.

Wang, C., Zhao, W., and Cui, Y.: Changes in the seasonally frozen ground over the eastern Qinghai-Tibet Plateau in the past 60 years. Frontiers in Earth Science, 8, 270. https://doi.org/10.3389/feart.2020.00270, 2020.

Wang, G., Liu, L. A., Liu, G., Hu, H., and Li, T.: Impacts of grassland vegetation cover on the active-layer thermal regime, northeast Qinghai-Tibet Plateau, China. Permafrost and Periglacial Processes, 21(4), 335-344. https://doi.org/10.1002/ppp.699, 2010.

Wang, T., Wu, T., Wang, P., Li, R., Xie, C., and Zou, D.: Spatial distribution and changes of permafrost on the Qinghai-Tibet Plateau revealed by statistical models during the period of 1980 to 2010. Science of the Total Environment, 650, 661-670. https://doi.org/10.1016/j.scitotenv.2018.08.398, 2019a.

Wang, T., Yang, D., Fang, B., Yang, W., Qin, Y., and Wang, Y.: Data-driven mapping of the spatial distribution and potential changes of frozen ground over the Tibetan Plateau. Science of The Total Environment, 649, 515-525. https://doi.org/10.1016/j.scitotenv.2018.08.369, 2019b.

Wang, X., Chen, R., Han, C., Yang, Y., Liu, J., Liu, Z., Guo S., and Song, Y.: Response of shallow soil temperature to climate change on the Qinghai-Tibetan Plateau. International Journal of Climatology, 41(1), 1-16. https://doi.org/10.1002/joc.6605, 2021.

Wang, X., Ran, Y., Pang, G., Chen, D., Su, B., Chen, R., Xin Li, X., Chen, H. W., Yang, M., Gou, X., Jorgenson, M. T., Aalto, J., Li, R., Peng, X., Wu, T., Clow, G. D., Wan, G., Wu, X., and Luo, D.: Contrasting characteristics, changes, and linkages of permafrost between the Arctic and the Third Pole. Earth-Science Reviews, 230, 104042. https://doi.org/10.1016/j.earscirev.2022.104042, 2022.

Xie, C., Zhao, L., Wu, T., and Dong, X.: Changes in the thermal and hydraulic regime within the active layer in the Qinghai-Tibet Plateau. J. Mt. Sci. 9, 483–491. https://doi.org/10.1007/s11629-012-2352-3, 2012.

Xu, X., and Wu, Q.: Active layer thickness variation on the Qinghai Tibetan Plateau: Historical and projected trends. Journal of Geophysical Research: Atmospheres, 126, e2021JD034841. https://doi.org/10.1029/2021JD034841, 2021.

https://doi.org/10.5194/egusphere-2024-1169
Preprint. Discussion started: 13 May 2024

Yao, T., Thompson, L., Yang, W.: Different glacier status with atmospheric circulations in Tibetan Plateau and surroundings. Nat Clim Change 2:663–667. https://doi.org/10.1038/nclimate1580, 2012.

485 You, Y., Guo, L., Yu, Q., Wang, X., Pan, X., Wu, Q., Wang, D., and Wang, G.: Spatial variability and influential factors of active layer thickness and permafrost temperature change on the Qinghai-Tibet Plateau from 2012 to 2018. Agricultural and Forest Meteorology, 318, 108913. https://doi.org/10.1016/j.agrformet.2022.108913, 2022.

Zhang, M., Wen, Z., Li, D., Chou, Y., Zhou, Z., Zhou, F., and Lei, B.: Impact process and mechanism of summertime rainfall on thermal–moisture regime of active layer in permafrost regions of central Qinghai–Tibet Plateau. Science of the

490 Total Environment, 796, 148970. https://doi.org/10.1016/j.scitotenv.2021.148970, 2021.

Zhao, D., and Wu, S.: Projected changes in permafrost active layer thickness over the Qinghai-Tibet Plateau under climate change. Water Resources Research, 55(9), 7860-7875. https://doi.org/10.1029/2019WR024969, 2019.

Zou, D., Zhao, L., Sheng, Y., Chen, J., Hu, G.J., Wu, T., Wu, J., Xie, C., Wu, X., Pang, Q., Wang, W., Du, E., Li, W., Liu, G., Li, J., Qin, Y., Qiao, Y., Wang, Z., Shi, J., and Cheng, G.: A new map of permafrost distribution on the Tibetan Plateau,

495 The Cryosphere, 11, 2527–2542, https://doi.org/10.5194/tc-11-2527-2017, 2017.